View metadata, citation and similar papers at core.ac.uk
brought to you by CORE

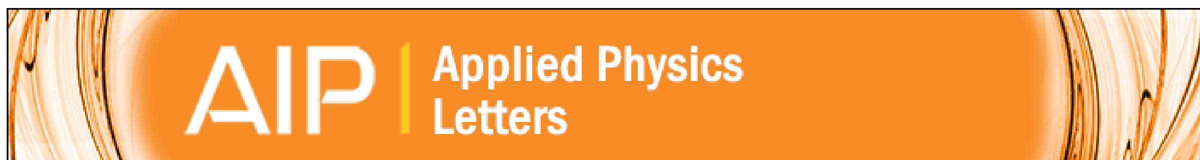

Two-dimensional mapping of triaxial strain fields in a multiferroic Bi Fe O 3 thin film using scanning x-ray microdiffraction

Chung W. Bark, Kyung C. Cho, Yang M. Koo, Nobumichi Tamura, Sangwoo Ryu, and Hyun M. Jang

Citation: Applied Physics Letters **90**, 102904 (2007); doi: 10.1063/1.2711530
View online: http://dx.doi.org/10.1063/1.2711530
View Table of Contents: http://scitation.aip.org/content/aip/journal/apl/90/10?ver=pdfcov
Published by the AIP Publishing

Articles you may be interested in

Role of defects in BiFeO3 multiferroic films and their local electronic structure by x-ray absorption spectroscopy
J. Appl. Phys. **116**, 153701 (2014); 10.1063/1.4898196

Enhanced magnetoelectric effect in La0.67Sr0.33MnO3/PbZr0.52Ti0.48O3 multiferroic nanocomposite films with a SrRuO3 buffer layer
J. Appl. Phys. **113**, 164106 (2013); 10.1063/1.4803057

Electric-field-induced structural modulation of epitaxial Bi Fe O 3 multiferroic thin films as studied using x-ray microdiffraction
Appl. Phys. Lett. **90**, 022902 (2007); 10.1063/1.2430678

Lattice strain in epitaxial Ba Ti O 3 thin films
Appl. Phys. Lett. **88**, 152908 (2006); 10.1063/1.2194231

Leakage current of multiferroic (Bi 0.6 Tb 0.3 La 0.1) Fe O 3 thin films grown at various oxygen pressures by pulsed laser deposition and annealing effect
J. Appl. Phys. **99**, 054104 (2006); 10.1063/1.2177430

You don't still use this cell phone
or this computer
Why are you still using an AFM designed in the 80's?
It is time to upgrade your AFM
Minimum $20,000 trade-in discount for purchases before August 31st
Asylum Research is today's technology leader in AFM
dropmyoldAFM@oxinst.com
OXFORD INSTRUMENTS
The Business of Science®

This article is copyrighted as indicated in the article. Reuse of AIP content is subject to the terms at: http://scitation.aip.org/termsconditions. Downloaded to IP: 141.223.173.110 On: Tue, 21 Apr 2015 11:07:34

APPLIED PHYSICS LETTERS **90**, 102904 (2007)

Two-dimensional mapping of triaxial strain fields in a multiferroic $BiFeO_3$ thin film using scanning x-ray microdiffraction

Chung W. Bark, Kyung C. Cho, and Yang M. Koo
Department of Materials Science and Engineering, Pohang University of Science and Technology (POSTECH), Pohang 790-784, Republic of Korea and Pohang Accelerator Laboratory (PAL), Pohang University of Science and Technology (POSTECH), Pohang 790-784, Republic of Korea

Nobumichi Tamura
Advanced Light Source (ALS), Lawrence Berkeley National Laboratory, Berkeley, California 94720

Sangwoo Ryu and Hyun M. Jang[a]
Department of Materials Science and Engineering, Pohang University of Science and Technology (POSTECH), Pohang 790-784, Republic of Korea and Pohang Accelerator Laboratory (PAL), Pohang University of Science and Technology (POSTECH), Pohang 790-784, Republic of Korea

(Received 15 December 2006; accepted 1 February 2007; published online 7 March 2007)

The dramatically enhanced polarizations and saturation magnetizations observed in the epitaxially constrained $BiFeO_3$ (BFO) thin films with their pronounced grain-orientation dependence have attracted much attention and are attributed largely to the constrained in-plane strain. Thus, it is highly desirable to directly obtain information on the two-dimensional (2D) distribution of the in-plane strain and its correlation with the grain orientation of each corresponding microregion. Here the authors report a 2D quantitative mapping of the grain orientation and the local triaxial strain field in a 250 nm thick multiferroic BFO film using a synchrotron x-ray microdiffraction technique. This direct scanning measurement demonstrates that the deviatoric component of the in-plane strain tensor is between 5×10^{-3} and 6×10^{-3} and that the local triaxial strain is fairly well correlated with the grain orientation in that particular region. © *2007 American Institute of Physics*.
[DOI: 10.1063/1.2711530]

Multiferroic ferroelectromagnets[1] that display simultaneous magnetic and polarization orderings have stimulated intense scientific and technological interest.[2–7] Among the many ferroelectromagnets, rhombohedral $BiFeO_3$ (space group $R3c$) is known to be the only perovskite material that exhibits multiferroism at room temperature with its ferroelectric Curie point of ~850 °C and antiferromagnetic Néel temperature of 370 °C.[8] Thus, $BiFeO_3$ (BFO) is currently considered to be the prime candidate for future device applications.

Recently, Wang *et al.*[2] fabricated epitaxial pseudotetragonal BFO films having a remanent polarization (P_r) almost an order of magnitude higher than that of bulk BFO by applying a strong compressive stress imposed by the bottom $SrRuO_3$ electrode. Though there are some controversial arguments,[9] the dramatically enhanced polarization and saturation magnetization in the distorted pseudotetragonal BFO thin film[2] are attributed largely to the constrained strain in the heteroepitaxially grown film layer.[2,10–13] In addition to this critical role of epitaxial film strain on the enhanced polarization and magnetization,[2,11–13] it has been reported that the value of P_r is highly susceptible to the grain orientation in a given BFO thin film.[10]

In view of these, it is very important to directly obtain information on the two-dimensional (2D) distribution of lattice strain and its correlation with the grain orientation of each corresponding microregion. The strain around ferroelectric domains has been observed by using various techniques including transmission electron microscopy,[14] atomic force microscopy,[15] and synchrotron scanning x-ray microdiffraction (S-XRMD).[16] However, only S-XRMD allows us a direct measurement of the strain fields around local ferroelectric domains or grains. Rogan *et al.*[16] carried out S-XRMD study using a $BaTiO_3$ single crystal. In spite of its importance, however, no direct measurement of the strain field in a multiferroic material has been performed prior to the present study. Here we report a first-of-its-kind 2D quantitative mapping of the grain orientation and local triaxial strain field in a BFO thin film using S-XRMD technique. This measured deviatoric component of the local triaxial strain (i.e., lattice distortion) was correlated with the grain orientation in that particular region.

Pulsed laser deposition (PLD) was employed to prepare a BFO thin film on a (001) plane of $SrTiO_3$ (STO). To examine the effect of the grain orientation on the local in-plane strain tensor, we have intentionally fabricated a BFO film with more than one grain orientation. Thus, the deposition conditions used in the present study were somewhat different from those used in the fabrication of [001]-oriented pseudotetragonal epitaxial BFO films.[11] The main differences are (1) the target composition, $Bi_{1.05}FeO_3$, (2) the deposition temperature, 675 °C, and (3) the oxygen partial pressure, 100 mTorr.

The x-ray diffraction (XRD) pattern indicated that the film was preferentially [001] oriented with some minor reflection peaks mostly from [101] reflection. As presented in Fig. 1, the pole figure confirms that the BFO thin film on (001) STO is preferentially grown along the [001] direction. However, one cannot ignore other grain orientations, especially [101]-type orientations. The degree of [001]-type preferred orientation, as estimated using the Lotgering orienta-

[a]Author to whom correspondence should be addressed; electronic mail: hmjang@postech.ac.kr

This article is copyrighted as indicated in the article. Reuse of AIP content is subject to the terms at: http://scitation.aip.org/termsconditions. Downloaded to IP: 141.223.173.110 On: Tue, 21 Apr 2015 11:07:34

 © 2007 American Institute of Physics

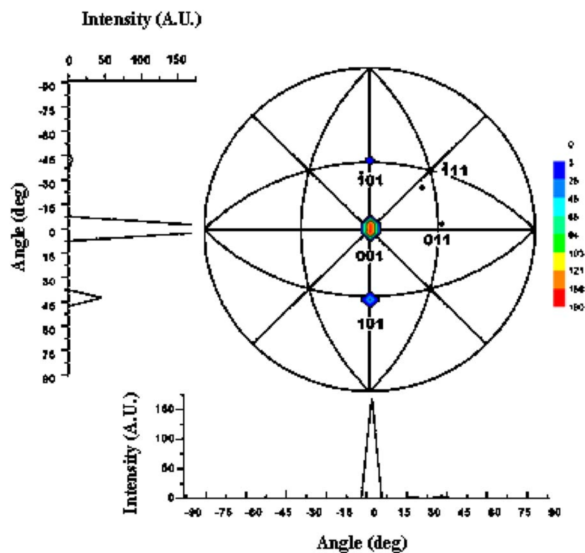

FIG. 1. (Color online) Pole figure of the 250 nm thick BFO film showing [001]-preferential growth.

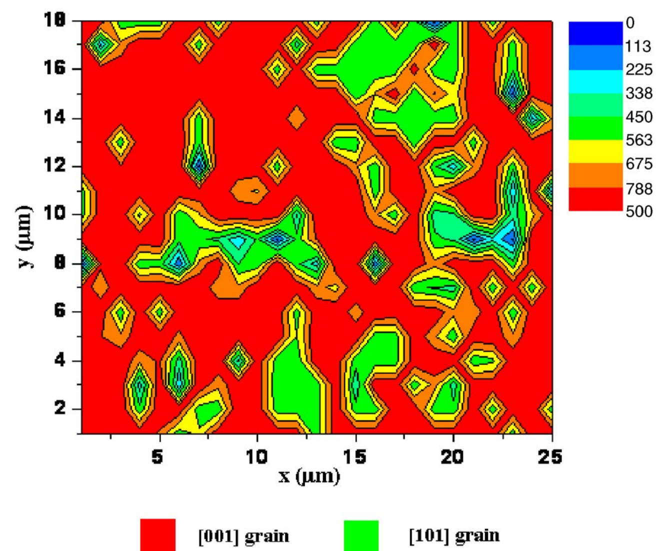

FIG. 2. (Color online) Two-dimensional mapping of the grain orientation in the 250 nm thick BFO film on (001) STO. The step size used in the present S-XRMD experiment is 1 μm, and the total scanned area is 25×18 μm^2. In the figure, x and y denote two orthogonal in-plane directions.

tion factor,[17] is ~75%. Polarized Raman scattering of the 500 nm thick [001] preferentially oriented BFO film by employing the side-view $Y(ZZ)Y'$ scattering configuration confirmed the three mode frequencies of the transverse optical A_1(TO) phonons for the tetragonal $P4mm$ BFO (Ref. 18) at 136, 168, and 212 cm^{-1}.

The polarization–electric field (P-E) curves of the 250 nm thick film capacitor fabricated on the bottom electrode structure of $SrRuO_3$ (50 nm)/STO showed that the net switching polarization ($2P_r$) measured at 1 kHz with $E_{max}=\pm 400$ kV/cm is 62 $\mu C/cm^2$. The M-H curves of the present PLD-grown BFO film with a mixed grain orientation were very similar to those of the [001]-oriented epitaxial pseudotetragonal BFO film having the same thickness of 250 nm.[19]

We now seek for detailed information on the spatial distribution of lattice distortions and its correlation with the grain orientations at each corresponding microregion in a constrained BFO film. For this purpose, the S-XRMD experiment was conducted on beamline 7.3.3 at the Advanced Light Source, Lawrence Berkeley National Laboratory. The energy of the polychromatic x-ray beam was between 5 and 14 keV, and the beam cross section was measured to be around 1×1 μm^2. A more detailed description of the beamline can be found in Ref. 20.

The data were analyzed with the x-ray microdiffraction analysis indexing software (XMAS) which adopts nonlinear least-squares refinement.[20] Geometrical calibration parameters were determined by using a single-crystal unstrained STO sample with its lattice parameter (a) of 3.905 Å. The grain orientation, i.e., (hkl)-peak indexing, of each scanned area (pixel) was determined by having the XMAS code search for proper sets to compare the theoretical scattering vector based on the local spin-density approximation[2] (LSDA) with the scattering vector from the experimental Laue reflection. Because the exact atomic positions for the present thin-film BFO phase with $P4mn$ tetragonal symmetry are not known, the computed atomic positions and lattice parameters (a=3.935 Å and c=3.998 Å) based on the LSDA (Ref. 2) were adopted in the computation of the theoretical scattering vector.

Exact values of the local strain tensor were obtained from the transformation matrix which in turn was evaluated from the unit-cell parameters of each scanned position and the input unstrained unit-cell parameters obtained from the LSDA result. Because the deviatoric strains involved the changes in the angles between atomic planes, the deviatoric tensor was evaluated from the angular displacements of the Laue spots in an experimental Laue pattern. In this way, the crystal orientation and the triaxial deviatoric strain tensor (ε'_{xx}) were obtained for every scanned position. The accuracy of measuring the deviatoric strain tensor (i.e., lattice distortion) depends on the number of Laue reflections used in the strain refinement.[21,22] In the present S-XRMD study, we evaluated the deviatoric strain tensor by employing more than 72 Laue reflections. According to Valek,[22] the uncertainty of our measurement of the deviatoric strain tensor is estimated to be essentially zero.

Figure 2 presents the 2D mapping of grain orientation, as

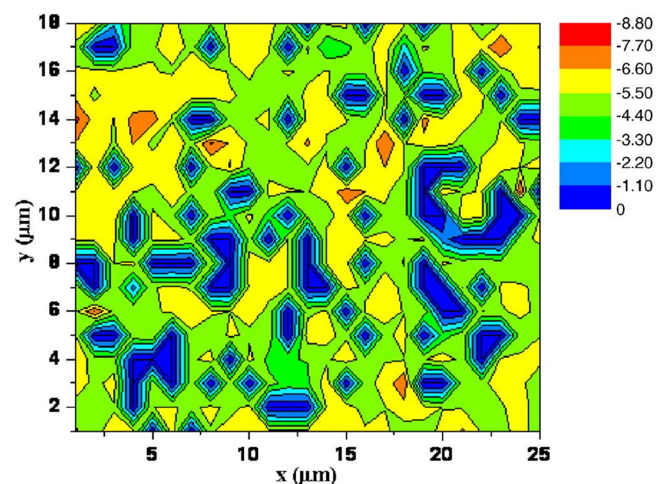

FIG. 3. (Color online) Two-dimensional spatial distribution of the deviatoric component of the in-plane residual strain in the 250 nm thick BFO film on (001) STO. Exact values of the local in-plane strain tensor, i.e., $(1/2)(\varepsilon'_{xx}+\varepsilon'_{yy})$, were obtained from the unit-cell parameters of each scanned position and the input unstrained unit-cell parameters.

This article is copyrighted as indicated in the article. Reuse of AIP content is subject to the terms at: http://scitation.aip.org/termsconditions. Downloaded to IP: 141.223.173.110 On: Tue, 21 Apr 2015 11:07:34

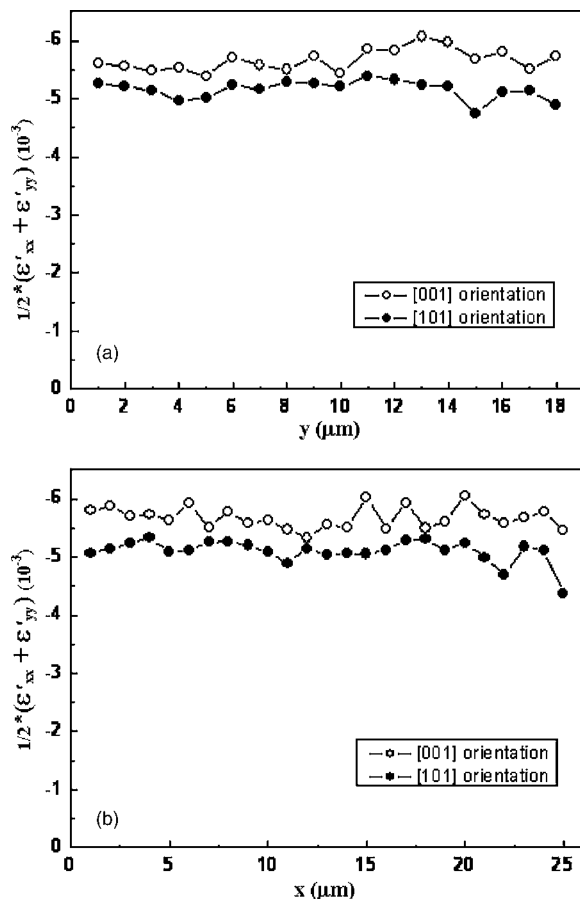

FIG. 4. Correlation between the local in-plane strain tensor and the grain orientation. (a) x-integrated average of the deviatoric component of the in-plane strain tensor for the two different grain orientations, plotted as a function of y. (b) y-integrated average of the deviatoric component of the in-plane strain tensor for the two different grain orientations, plotted as a function of x.

obtained using the method of S-XRMD. The red-colored region denotes the [001]-oriented grains, whereas the green-colored regions scattered in the matrix of [001]-oriented grains represent the [101]-oriented grains. Besides these two major orientations, a negligible portion of the scanned area actually corresponds to the grains with higher (hkl) indices, mostly $[\bar{1}11]$. This region is marked with a deep blue color. The (hkl) indexing of each scanned microregion ($1\times 1\ \mu m^2$) indicates that ~65% of the scanned area in Fig. 2 consists of [001]-oriented grains and ~20% corresponds to [101]-oriented grains. These estimates exclude the yellow- and orange-colored transition regions located between the [001]- and [101]-oriented domains.

Figure 3 represents a 2D spatial distribution of the deviatoric component of the in-plane residual strain tensor. We have plotted the sum of ε'_{xx} and ε'_{yy} instead of ε'_{xx} (or ε'_{yy}) alone since $(1/2)(\varepsilon'_{xx}+\varepsilon'_{yy})$ [i.e., $-(1/2)\varepsilon'_{zz}$] is the most appropriate measure of the in-plane strain, where z denotes the out-of-plane direction which is normal to x and y. Various colors shown in the right-hand-side column of Fig. 3 represent different values of the deviatoric strain tensor $[-(1/2)\varepsilon'_{zz}\times 10^{-3}]$. Thus, the maximum observed in-plane residual strain is as large as -8.8×10^{-3}. Comparing the in-plane strain mapping (Fig. 3) with the 2D distribution of grain orientations (Fig. 2), one can notice that the lattice distortion is more pronounced in the region of [001]-oriented grains in general.

A quantitative correlation between the local in-plane strain tensor and the grain orientation can be made by plotting the in-plane strain tensor along any of the two orthogonal in-plane directions. Figure 4(a) shows the x-integrated average of the deviatoric component of the in-plane strain tensor for the two major grain orientations, plotted as a function of y. Similarly, Fig. 4(b) presents the grain-orientation dependence of the y-integrated average of the in-plane strain tensor for various locations of x. As presented in Fig. 4, the residual strain of the [001]-oriented grain is consistently larger than that of the [101]-oriented grain throughout the whole region, showing a fairly good correlation between these two structural parameters. The present S-XRMD result is also consistent with the recent report[10] obtained by using conventional XRD that the monoclinically distorted BFO film heteroepitaxially grown on (001) STO is under more significant epitaxial constraint than the film grown on (101) STO.

This work was supported by the Korea Science and Engineering Foundation (KOSEF) under Contract No. R01-2005-000-10354-0. The authors thank B. C. Valek for his assistance in performing x-ray microdiffraction experiments at the Advanced Light Source (ALS), Lawrence Berkeley National Laboratory (LBNL), USA. The ALS is supported by the Director, Office of Science, Office of Basic Energy Sciences, of the U.S. Department of Energy under Contract No. DE-AC02-05CH11231.

[1]N. A. Hill, J. Phys. Chem. B **104**, 6694 (2000).
[2]J. Wang, J. B. Neaton, H. Zheng, V. Nagarajan, S. B. Ogale, B. Liu, D. Viehland, V. Vaithyanathan, D. G. Schlom, U. V. Waghmare, N. A. Spaldin, K. M. Rabe, M. Wuttig, and R. Ramesh, Science **299**, 1719 (2003).
[3]T. Kimura, T. Goto, H. Shintani, K. Ishizaka, T. Arima, and Y. Tokura, Nature (London) **426**, 55 (2003).
[4]H. Zheng, J. Wang, S. E. Lofland, Z. Ma, L. Mohaddes-Ardabili, T. Zhao, L. Salamanca-Riba, S. R. Shinde, S. B. Ogale, F. Bai, D. Viehland, Y. Jia, D. G. Schlom, M. Wuttig, A. Roytburd, and R. Ramesh, Science **303**, 661 (2004).
[5]N. Hur, S. Park, P. A. Sharma, J. S. Ahn, S. Guha, and S. W. Cheong, Nature (London) **429**, 392 (2004).
[6]T. Lottermoser, T. Lonkai, U. Amann, D. Hohlwein, J. Ihringer, and M. Fiebig, Nature (London) **430**, 541 (2004).
[7]N. Ikeda, H. Ohsumi, K. Ohwada, K. Ishii, T. Inami, K. Kakurai, Y. Murakami, K. Yoshii, S. Mori, Y. Horibe, and H. Kito, Nature (London) **436**, 1136 (2005).
[8]G. A. Smolenskii and I. E. Chupis, Sov. Phys. Usp. **25**, 475 (1982).
[9]W. Eerenstein, F. D. Morrison, J. Dho, M. G. Blamire, J. F. Scott, and N. D. Mathur, Science **307**, 1203a (2005).
[10]J. Li, J. Wang, M. Wuttig, R. Ramesh, N. Wang, B. Ruette, A. P. Pyatakov, A. K. Zvezdin, and D. Viehland, Appl. Phys. Lett. **84**, 5261 (2004).
[11]D. Lee, M. G. Kim, S. Ryu, H. M. Jang, and S. G. Lee, Appl. Phys. Lett. **86**, 222903 (2005).
[12]Q. Jiang and J. H. Qiu, J. Appl. Phys. **99**, 103901 (2006).
[13]F. Bai, J. Wang, M. Wuttig, J. Li, N. Wang, A. P. Pyatakov, A. V. Zvezdin, L. E. Cross, and D. Viehland, Appl. Phys. Lett. **86**, 032511 (2005).
[14]G. Arlt, D. Hennings, and G. Dewith, J. Appl. Phys. **58**, 1619 (1985).
[15]J. Muñoz-Saldaña, G. A. Schneider, and L. M. Eng, Surf. Sci. **480**, L402 (2001).
[16]R. C. Rogan, N. Tamura, G. A. Swift, and E. Üstündag, Nat. Mater. **2**, 379 (2003).
[17]F. K. Lotgering, J. Inorg. Nucl. Chem. **9**, 113 (1959).
[18]M. K. Singh, S. Ryu, and H. M. Jang, Phys. Rev. B **72**, 132101 (2005).
[19]C. W. Bark, S. Ryu, Y. M. Koo, H. M. Jang, and H. S. Youn, Appl. Phys. Lett. **90**, 022902 (2007).
[20]N. Tamura, R. S. Celestre, A. A. MacDowell, H. A. Padmore, R. Spolenak, B. C. Valek, N. M. Chang, A. Manceau, and J. R. Patel, Rev. Sci. Instrum. **73**, 1369 (2002).
[21]J. S. Chung and G. E. Ice, J. Appl. Phys. **86**, 5249 (1999).
[22]B. C. Valek, Ph.D. thesis, Stanford University, 2003.

This article is copyrighted as indicated in the article. Reuse of AIP content is subject to the terms at: http://scitation.aip.org/termsconditions. Downloaded to IP: 141.223.173.110 On: Tue, 21 Apr 2015 11:07:34